# REPORT DOCUMENTATION PAGE

*Form Approved*
*OMB No. 0704-0188*

Public reporting burden for this collection of information is estimated to average 1 hour per response, including the time for reviewing instructions, searching existing data sources, gathering and maintaining the data needed, and completing and reviewing this collection of information. Send comments regarding this burden estimate or any other aspect of this collection of information, including suggestions for reducing this burden to Department of Defense, Washington Headquarters Services, Directorate for Information Operations and Reports (0704-0188), 1215 Jefferson Davis Highway, Suite 1204, Arlington, VA 22202-4302. Respondents should be aware that notwithstanding any other provision of law, no person shall be subject to any penalty for failing to comply with a collection of information if it does not display a currently valid OMB control number. **PLEASE DO NOT RETURN YOUR FORM TO THE ABOVE ADDRESS.**

| 1. REPORT DATE *(DD-MM-YYYY)* | 2. REPORT TYPE | 3. DATES COVERED *(From - To)* |
|---|---|---|
| 02-07-2012 | Conference Paper | |

**4. TITLE AND SUBTITLE**

**Investigation of Singly Ionized Iodine Spectroscopy in Support of Electrostatic Propulsion Diagnostics Development**

**5a. CONTRACT NUMBER**

**5b. GRANT NUMBER**

**5c. PROGRAM ELEMENT NUMBER**

**6. AUTHOR(S)**
Hargus Jr., W.A.; Lubkeman, J.S.; Remy, K.E.; Gonzales, A.E.

**5d. PROJECT NUMBER**

**5f. WORK UNIT NUMBER**
23080535

**7. PERFORMING ORGANIZATION NAME(S) AND ADDRESS(ES)**

Air Force Research Laboratory (AFMC)
AFRL/RZSS
1 Ara Drive
Edwards AFB CA 93524-7013

**8. PERFORMING ORGANIZATION REPORT NUMBER**

**9. SPONSORING / MONITORING AGENCY NAME(S) AND ADDRESS(ES)**

Air Force Research Laboratory (AFMC)
AFRL/RQR
5 Pollux Drive
Edwards AFB CA 93524-7048

**10. SPONSOR/MONITOR'S ACRONYM(S)**

**11. SPONSOR/MONITOR'S NUMBER(S)**
AFRL-RZ-ED-TP-2012-228

**12. DISTRIBUTION / AVAILABILITY STATEMENT**

Approved for public release; distribution unlimited (PA #12508).

**13. SUPPLEMENTARY NOTES**
For presentation at the 48th AIAA/ASME/SAE/ASEE Joint Propulsion Conference & Exhibit and 10th International Energy Conversion Engineering Conference, Atlanta, GA, 29 July- 2 August 2012

**14. ABSTRACT**

This effort examines the spectroscopy of the second spectrum of the iodine atom (I II) in order to determine one, or more, useful transitions for laser-induced fluorescence of an accelerated atomic iodine singly charged ion (I+). While the second spectrum of iodine has been analyzed, it is not particularly well characterized. Nor has it been studied substantially within a plasma such as those of interest to the spacecraft propulsion community. Our goal is to examine the spectral data available in the literature and determine transitions suitable for development into diagnostics tools, such as laser-induced fluorescence (LIF), to examine the plasma acceleration within an electro-static plasma propulsion thruster. While xenon remains the preferred propellant for electro-static spacecraft propulsion, a number of alternative propellants are being analyzed in various laboratories. Some of the propellants that have been investigated in the recent literature include krypton, bismuth, and iodine. Of these alternative propellant candidates, iodine is the least well investigated. However, due to its close mass (127 versus 131 amu) compared to xenon, it has strong potential for use as an electro-static propulsion propellant. Iodine's benefits include a solid density of 4.9 g/cc, a low boiling point of 183 _C. Compared to xenon storage density of 1.2 g/cc at 2,000 psi, or the bismuth boiling point of 1,564 _C, there appear to be system level advantages to iodine fueled electrostatic spacecraft propulsion. This effort focuses on the development of a laser-induced fluorescence diagnostic tool for the iodine ion.

**15. SUBJECT TERMS**

| 16. SECURITY CLASSIFICATION OF: | | | 17. LIMITATION OF ABSTRACT | 18. NUMBER OF PAGES | 19a. NAME OF RESPONSIBLE PERSON |
|---|---|---|---|---|---|
| | | | | | W.A. Hargus Jr. |
| a. REPORT | b. ABSTRACT | c. THIS PAGE | | | 19b. TELEPHONE NUMBER *(include area code)* |
| **Unclassified** | **Unclassified** | **Unclassified** | SAR | 11 | N/A |

# Investigation of Singly Ionized Iodine Spectroscopy in Support of Electrostatic Propulsion Diagnostics Development

William A. Hargus, Jr.*
Jordan S. Lubkeman†
Kahli E. Remy‡
Ashley E. Gonzales§
*Air Force Research Laboratory, Edwards Air Force Base, CA 93524*

**This effort examines the spectroscopy of the second spectrum of the iodine atom (I II) in order to determine one, or more, useful transitions for laser-induced fluorescence of an accelerated atomic iodine singly charged ion ($I^+$). While the second spectrum of iodine has been analyzed, it is not particularly well characterized. Nor has it been studied substantially within a plasma such as those of interest to the spacecraft propulsion community. Our goal is to examine the spectral data available in the literature and determine transitions suitable for development into diagnostics tools, such as laser-induced fluorescence (LIF), to examine the plasma acceleration within an electro-static plasma propulsion thruster. While xenon remains the preferred propellant for electrostatic spacecraft propulsion, a number of alternative propellants are being analyzed in various laboratories. Some of the propellants that have been investigated in the recent literature include krypton, bismuth, and iodine. Of these alternative propellant candidates, iodine is the least well investigated. However, due to its close mass (127 versus 131 amu) compared to xenon, it has strong potential for use as an electro-static propulsion propellant. Iodine's benefits include a solid density of 4.9 g/cc, a low boiling point of 183 °C. Compared to xenon storage density of 1.2 g/cc at 2,000 psi, or the bismuth boiling point of 1,564 °C, there appear to be system level advantages to iodine fueled electrostatic spacecraft propulsion. This effort focuses on the development of a laser-induced fluorescence diagnostic tool for the iodine ion.**

## Introduction

At present, xenon (Xe) is the propellant of choice for most electrostatic plasma thrusters including Hall effect thrusters. The selection of xenon is due to a number of rigorous engineering rationale. These include the high mass (131 amu) and relatively low ionization potential (12.1 eV) of xenon; as well as the inert nature of xenon, which eliminates much of the controversy that plagued early electrostatic propulsion efforts when mercury (Hg) and cesium (Cs) were the propellants of choice.[1] Although xenon is a noble gas, it is the most massive stable such element, and due to its non-ideal gas behavior, it is possible to pressurize and store with room temperature specific densities approaching 1.2.[2,3] As such, it may be stored at higher densities than that of the most common liquid monopropellant, hydrazine, which has a specific gravity of 1.02.

*Senior Engineer, AFRL/RZSS, Edwards AFB, CA, USA.
†Engineering Intern, AFRL/RZSS, Edwards AFB, CA, USA.
‡Engineering Physicist, ERC, Inc., Edwards AFB, CA, USA.
§Engineer AFRL/RZSS, Edwards AFB, CA, USA.

### Propellant Selection

While xenon is an excellent propellant for electrostatic thrusters with significant ground test and flight heritage, there are several concerns that have driven the Hall effect thruster community to explore alternative propellants. As orbit raising missions of longer duration and larger payloads are proposed, requisite propellant mass increases dramatically. Xenon production is a byproduct of the fractional distillation of atmospheric gases for use primarily by the steel industry. Due to the low concentration of xenon in the atmosphere (∼90 ppb), worldwide production is only approximately 6,000 standard cubic meters per year. Increasing industrial demand for items such as high efficiency lighting and windows, as well as plasma based micro-fabrication, has produced wide price swings in the past decade. Xenon prices have varied by as much as factor of ten in the past decade.

Krypton (Kr) has been examined as an alternative to xenon and is used in several academic laboratories as a less expensive substitute to xenon. Krypton has a lower atomic mass (83.8 amu), but a slightly higher ionization potential (14.0 eV) than xenon.[2] Like xenon, krypton is a noble gas and could be easily integrated into existing Hall effect thruster propellant management systems without much modification. One



DISTRIBUTION A: Distribution Unlimited.

significant issue is the storage density of gaseous krypton is lower than xenon due to krypton's higher critical temperature. The lower storage density coupled with the lower efficiency of krypton propellant due to lower residence time and lower ionization cross-section has to date precluded flights of krypton fueled electrostatic thrusters. However, the 6× lower cost (by mass) of krypton relative to xenon remains intriguing.[4,5,6] Recent studies have examined the possibility of cryogenic storage of krypton as a method to reduce the tankage fraction to approximately 1%.[3] This propellant architecture would be advantageous for large scale space tug applications, but would be difficult to implement for more conventional missions such as station–keeping for GEO communications satellites.

Bismuth (Bi) was studied extensively as a possible propellant for electrostatic thrusters due to its high mass (209 amu), low ionization energy (7.29 eV), and high density (solid density of 9.78 g/cc).[2] While the melting point of bismuth is relatively low at 272 °C, the boiling point is 1,564 °C. Vapor pressures of 100 Pa require a temperature of 892 °C. While a number of experimental efforts were very successful in the laboratory in developing bismuth Hall effect thrusters, the high temperatures involved necessitated heroic efforts in the engineering of propellant feed systems. Ultimately, interest in bismuth as an electrostatic thruster propellant has declined in no small part due to the high temperatures required for successful propellant feed implementation. Unfortunately, the ultimate hurdle is most likely the fact that the spacecraft community remains highly skeptical of any propulsion system with the potential to coat the host spacecraft with a low vapor pressure metal.

Iodine ($I_2$) has been discussed seriously as a propellant for Hall effect thrusters as early as 2000.[7,8] Atomic iodine has a mass of 126.9 amu, but as a halogen the natural state is diatomic ($I_2$) with a molecular mass of 253.8 amu. Atomic iodine has an ionization energy of only 10.45 eV. The density of iodine (solid at room temperature) is 4.933 g/cc. Iodine has a relatively high vapor pressure at low temperatures. Vapor pressures of 100 Pa are achieved at 39°C. It appears obvious that the spacecraft community will benefit from a propellant with nearly the atomic characteristics as xenon, but with a lower ionization potential. In addition, iodine is approximately 100× less expensive and more abundant than xenon while exhibiting better gasification characteristics than bismuth. Iodine appears to offer the benefits of cryogenic propellant storage without the need for active cooling or insulation, and only a moderate heating requirement for gasification (183 °C yields 1 atm iodine pressure). A propellant storage system for iodine would likely have mass fractions of less than 1%. Table 1 summarizes the properties of xenon, krypton, bismuth, and iodine that have relevance to the propulsion engineer.[2]

**Table 1 Comparison of properties critical for electrostatic propulsion for various propellants.[2]**

| Property | Units | Xe | Kr | Bi | I |
|---|---|---|---|---|---|
| Atomic Mass | amu | 131.3 | 83.8 | 209 | 126.9 |
| $1^{st}$ Ion. Pot. | eV | 12.1 | 14.0 | 7.3 | 10.5 |
| $2^{nd}$ Ion. Pot. | eV | 21 | 24 | 16.7 | 19.1 |
| Stable Isotopes | | 9 | 6 | 1 | 1 |
| Odd Isotopes | | 2 | 1 | 1 | 1 |
| Den. (3000 psi) | g/cc | 1.11 | 0.91 | 9.78 | 4.93 |
| 100 Pa Pressure | °C | -170 | -199 | 892 | 39 |

### Iodine Electrostatic Thrusters

Although first proposed as a propellant by Dressler, et al. in 2000,[7] iodine has only been demonstrated using a Hall effect thruster in the laboratory in a very limited fashion. Initial testing of iodine has occurred at Busek, Co., Inc. (Natick, MA), with participation by the Air Force Institute of Technology (AFIT) and some support from the Air Force Research Laboratory (AFRL).[9,10] The nature of these studies has been exploratory and has concentrated on measurements of a xenon Hall effect thruster modified for operation using iodine as the propellant through the anode discharge. Published results show that iodine produces similar performance to xenon. The delivered specific impulse is generally slightly lower for iodine (typically 50 s lower); however, the thrust to power ratio, $T:P$, of iodine appears to be higher for iodine than xenon and increases with discharge potential. At 300 V anode potential, iodine produced a 15% higher $T:P$ value than xenon. It should be noted that the peak $T:P$ for xenon occurred at 250 V anode potential at a value equivalent to iodine. The $T:P$ value of iodine continued to increase and no maximum was identified within the 300 V anode potential upper limit of the study.

While the laboratory evaluations of iodine in an operational electrostatic plasma thruster are limited, the results are very promising. Performance appears to be on par with xenon without significant modification of the thruster. Intriguingly, performance appears to rise and exceed xenon at higher discharge potentials. The extent to which these behaviors continue above the limits of the initial studies is unknown, but is under active investigation. Present work at Busek is focused on construction of a full system to demonstrate a iodine Hall effect thruster system.

All of these issues must be addressed to determine potential performance gains over state of the art xenon thrusters and potential spacecraft interactions. While many of the probe based diagnostics customarily used to diagnose the plumes of plasma thrusters can and



DISTRIBUTION A: Distribution Unlimited.

have provided valuable insights into iodine thruster plasma acceleration; optical diagnostics can provide unparalleled non-intrusive resolution of the plasma acceleration with sub-mm resolution.

As iodine is diatomic, it has a tendency to form molecular ions and charged clusters. In fact, the energy required to ionize $I_2$ is less than that required to ionize atomic iodine (I).[10] This leads to a significantly more complex plasma, both chemically and kinetically. As a result, significant effort will have to be expended to characterize and fundamentally understand propellant acceleration and the resulting species. In order to assess whether the potential advantages of iodine propellant can be realized in Hall effect thrusters and other electrostatic thruster types, experimental measurements of these plasmas must be obtained. Both to determine relative figures of functional merit, and for numerical simulation validation for increased fundamental understanding of subtle propellant effects. Many diagnostics previously developed for xenon plasmas can be applied with little modification. These include critical performance measures (e.g. thrust measurements using inverted pendulum thrust stands) and most electrostatic probes for far–plume characterization (e.g. Faraday probes for ion flux measurements, retarding potential analyzers for ion energy distributions, etc.). However, optical measurements such as laser-induced fluorescence, which can provide spatially resolved velocity distribution measurements, are species dependent and require significant retooling when applied to new propellants. This work examines theoretical development of laser-induced fluorescence of a iodine ion transition for application to measuring the ionization and acceleration of iodine plasmas. Our goal is to lay a foundation for the development of laser–induced fluorescence of the atomic iodine ion ($I^+$, aka I II) with the eventual goal of demonstration measurements in an iodine Hall effect thruster.

## Iodine Ion Spectroscopy

Iodine has a more complex plume chemistry than noble gases traditionally used as Hall effect thruster propellants. The molecular iodine ionization path of $I_2 + e \rightarrow I_2^+ + 2e$ only requires 9.4 eV, while the atomic iodine ionization path of $I + e \rightarrow I^+ + 2e$ requires 10.5 eV.[10] If molecular ions are formed, then some portion of the iodine propellant may have an effective mass of 254 amu. Such high molecular weights could account for increased $T : P$, some of which may have already been seen in the preliminary studies.[9,10] In order to well characterize the plasma acceleration by an electrostatic plasma thruster, interrogation of each of the dominate positive ion species ($I^+$, $I_2^+$, and perhaps higher charged ions), the neutral species ($I_2$ and I), and possibly negative ions (note that iodine is highly electro-negative) appear to be of interest. At this time, $I^+$ is presumed to be the species of greatest interest. As the $I_2$ dissociation energy is 1.54 eV and the electron temperature ($T_e$) within a Hall effect thruster discharge is in a range of 20–30 eV,[11] we anticipate that singly charged atomic ions will be the dominant heavy species.

The specific long and near-term goals of this effort are to identify a useful transition for atomic iodine ions ($I^+$), verify that the relevant electronic states are suitably populated, understand the details of the selected transition so that it may be used to diagnose the thruster plasma, verify the iodine ion transition using table top plasma apparatus, and finally transition this diagnostic technique to measuring the propellant acceleration using laser-induced fluorescence in the near plume and within an iodine Hall effect thruster as a demonstration of this diagnostic technique. In this paper, we present the spectroscopy studies and development of a table top apparatus.

### Transition Selection

Selecting a transition for LIF in low density, partially ionized plasma such as that in the near–field of a Hall effect thruster is primarily constrained by two factors. First, the probed energy level must have a sufficient population to produce substantial signal. Second, the transition wavelength must be laser accessible.

The ground state is usually inaccessible for routine laboratory diode laser based measurements. LIF measurements generally use Rydberg states with relatively large populations. As ion densities of Hall effect plasmas are seldom higher than $10^{18}$ $m^3$, collisional de-excitation of excited states is slow. Therefore, metastable states are generally highly populated, as they have no allowed radiative decay path. Once identified, metastable states are ideal lower states for laser probing. It also should be noted that non-metastable states may be used for LIF; however, this significantly reduces signal strength.[12]

Tunable lasers of three general types may be applied to plasma LIF. Dye lasers are the traditional source of tunable lasers for plasma and combustion work. These lasers remain workhorses, but suffer from complex user interactions due to the use of liquid lasing medium with finite lifetime. Solid state lasers such as titanium sapphire (Ti:Sapphire) and alexandrite lasers have similar system complexity, but use a solid state lasing medium. Both these types of lasers can be challenging to work with, but often provide unique capabilities especially with regard to wavelength range and high power outputs. The more recent arrival on the scene is the tunable diode laser. Diode lasers are generally limited to the red and near IR, but there are some limited semiconductor band gaps producing systems in the blue and near ultraviolet (UV). Despite their relatively low power (usually <100 mW and more often <10 mW), these laser systems have repeatedly



DISTRIBUTION A: Distribution Unlimited.

demonstrated the ability to produce nearly turnkey LIF systems. In addition, tunable diode laser systems are 10 to 100 times less expensive than the more capable, but much more difficult to maintain tunable dye laser systems. These practical considerations require identification of metastable states of quantum mechanically relatively complex atomic ions and limit wavelengths to the red and near infrared (NIR).

The initial, and only known, survey of the second spectrum of atomic iodine was performed by Martin and Corliss in 1960.[13] To our knowledge no further surveys of the $I^+$ spectrum have been performed. Our identification of the metastable states began by examining the 41 lowest energy states of $I^+$ as identified by Martin and Corliss. These correspond to ion energies between 0 and 103,101.57 $cm^{-1}$. The energy differences between all of these states were numerically calculated and the energy differences were calculated between each state and any other states with lesser energies. The tabulated wavelength tables were then consulted and each energy difference matched to identified $I^+$ wavelengths, if it existed. Using this technique, an energy level diagram was constructed with the specified goal of discovering any metastable states, as these do not have radiative relaxation paths to lower states.

From our study, two states were identified as metastable. These are the $5d^5D_4^o$ state at 86,036.32 $cm^{-1}$ and the $5d^3G_4^o$ at state 101,157.79 $cm^{-1}$. Both of these states have been recently confirmed as metastable by NIST in their newly updated compilation of atomic spectra.[14] Of these two identified metastable states, we have chosen to concentrate on $5d^5D_4^o$ at 86,036.32 $cm^{-1}$ as it is lower energy and should be more readily populated by radiative decay. Figure 1 shows the energy level diagram for the first 15 levels and identifies the $5d^5D_4^o$ as not exhibiting any observed radiative decay paths.

We identified $5d^5D_4^o$ state transitions to $6p^5P_3$ at 695.878 nm, $5d^3P_2^o$ at 351.432 nm, and $5d^3D_3^o$ at 823.520 nm. Of these optical transitions, the $5d^5D_4^o$–$6p^5P_3$ transition at 695.878 nm was characterized by Martin and Corliss as the strongest emission feature by 50×.[13] In this transition, the upper $5p^5P_3$ state has five additional decay paths, three of which are strong. These are at 540.542 nm to $5p^5\ ^3P_2^o$, 681.257 nm to $5d^5D_3^o$, and 516.12 nm to $6s^5S_2^o$. The first two transitions are both similar magnitude and measured by Martin and Corliss to be 3-5× stronger than either the $5p^5\ ^3P_2^o$–$6p^5P_3$ at 540.542 nm or $5d^5D_4^o$–$6p^5P_3$ at 695.878 nm transition in emission. Figure 2 shows the $I^+$ transitions centered about the $6p^5P_3$ state.

From this analysis, we believe that it is possible to excite the $5d^5D_4^o$–$6p^5P_3$ transition at 695.878 nm, and collect non-resonant emission from either the $5d^5D_3^o$–$6p^5P_3$ transition at 681.257 nm, or the $6s^5S_2^o$–$6p^5P_3$ transition at 516.12 nm. Due to the fact that the

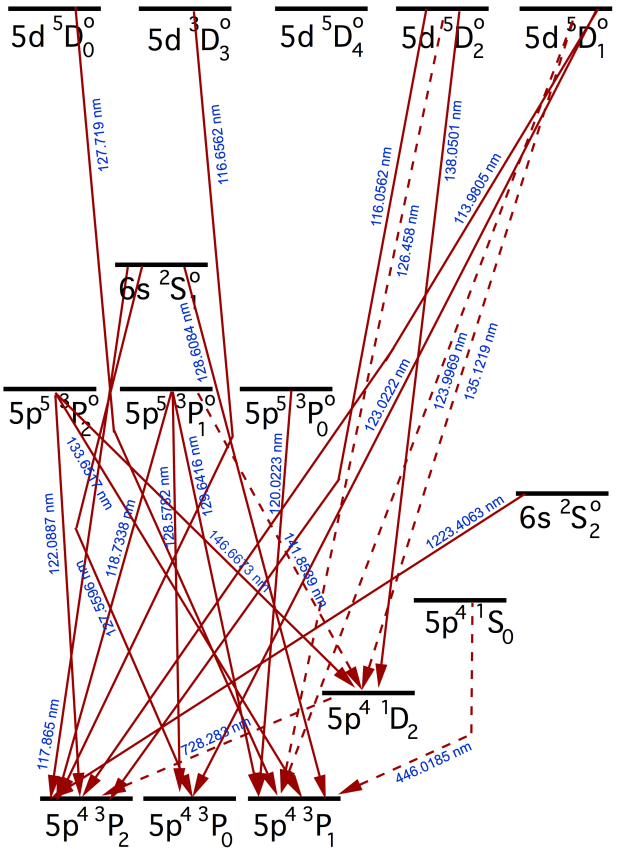


**Fig. 1 Energy level diagram for the first 15 states of the second spectrum of iodine where the $5d^5D_4^o$ state does not exhibit any radiative decay paths. Note that weak transitions are denoted by dashed lines.**

$5d^5D_4^o$ state is metastable, we anticipate that there will be substantial population for excitation. As the lowest lying metastable state, it will have the highest such population.

Without dedicated lifetime measurements and only using the Martin and Corliss' measured intensities, the branching ratio of the $6p^5P_3$ state to the $5d^5D_3^o$ is approximated to be in the neighborhood of 45% and to the $6s^5S_2^o$ state to be about 35%. Experimental studies will determine which transition is, if either, favored, but it should be noted that the quantum efficiency of a photomultiplier tube detector is higher at 516.12 nm.

### Laser-Induced Fluorescence

Laser-induced fluorescence (LIF) may be used to detect velocity–induced shifts in the spectral absorption of various plasma species. The fluorescence is monitored as a continuous-wave laser is tuned in frequency over the transition of interest, of energy $h\nu_{12}$, where $h$ is Plank's constant, $\nu_{12}$ is wavenumber of transition between lower state 1 and higher energy state 2. Note that state 1 may be the ground state, but any sufficiently highly populated excited state will do. For the highly excited, but low density accelerated



DISTRIBUTION A: Distribution Unlimited.

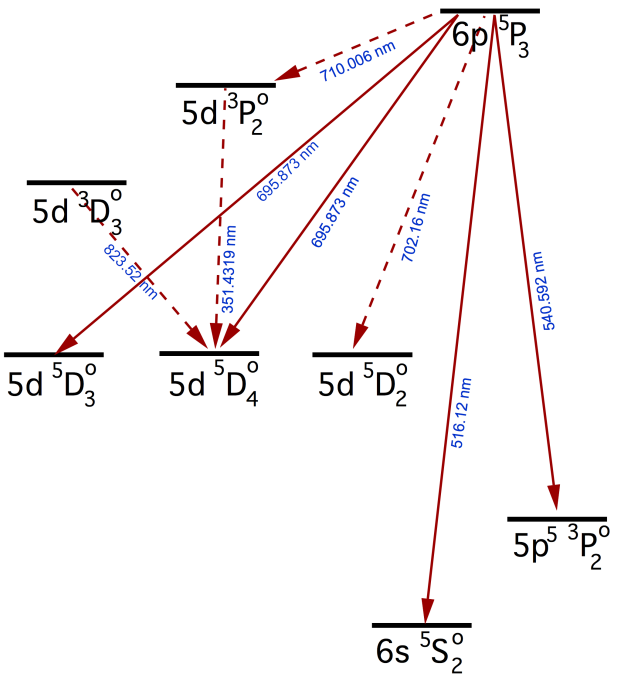


**Fig. 2 Second spectrum of iodine about the $6p^5P_3$ state. Note that weak transitions are denoted by dashed lines.**

plasmas of interest, we generally choose to examine a metastable state to ensure highest signal levels at convenient excitation wavelengths. Measurements can be made with high spatial resolution as determined by the intersection of probe laser beam with fluorescence optical collection.

Velocity measurements may be made using LIF velocimetry as an atomic, or as in our case an ionic, population moving with a velocity component $u$ relative to the direction of the incoming laser absorbs photons at a frequency shifted from that of stationary absorbers due to the Doppler effect. The magnitude of this frequency shift $\delta\nu_{12}$ is

$$\delta\nu_{12} = \frac{u}{c}\nu_{12}. \tag{1}$$

The measured fluorescence lineshape is determined by the environment of the absorbing ion population, so an accurate measurement of the lineshape function may lead to the determination of a number of plasma parameters beyond simple bulk velocities. The precision of measured velocities has been found, in various studies, to be less than the experimental uncertainty for the ions ($\pm$500 m/s).[15,16,17]

Several factors affect the lineshape and give rise to broadening and/or a shift of the spectral line. In high-temperature plasmas, the most significant is Doppler broadening due to the absorber's random thermal motion, characterized by the atomic, or ionic, kinetic temperature, $T_{kin}$. When the absorbing species velocity distribution is Maxwellian in shape, the Doppler broadening results in a Gaussian lineshape. Collisional interactions between the absorbers and other species in the plasma give rise to spectral lineshapes that are often Lorentzian. This includes interactions with charged particles (Stark broadening) and uncharged particles (van der Waals broadening). If both Doppler broadening and collisional broadening are important and independent, the resulting lineshape is a convolution of the Gaussian and Lorentzian lineshape into a Voigt lineshape.[18]

LIF is a convenient diagnostic for the investigation of ion velocities in a plasma thruster as it does not physically perturb the discharge. The LIF signal is a convolution of the velocity distribution function (VDF), transition lineshape, and laser beam frequency profile. Determination of the VDF from LIF data only requires the deconvolution of the transition lineshape and laser beam profile from the raw LIF signal trace. Alternatively, the lineshape itself may also provide valuable information on the state of the plasma, such as electron density, pressure, or heavy species temperature. In the somewhat turbulent plasmas typical of Hall effect thrusters, the fluorescence lineshape can also be indicative of the relative motion of the ionization zone as it axially traverses in the periodic breathing mode plasma fluctuation.[19,20] However, care must be taken to ensure that the relative effects of these phenomena are separable. In addition, magnetic (Zeeman effect) and electric (Stark effect) fields may also influence the fluorescence lineshape[21] and must be accounted for when analyzing the lineshapes should the fields be of sufficient magnitude. In the case of LIF of ions in a Hall effect thruster, the fluorescence lineshape appears to be most indicative of the aforementioned plasma turbulence including periodicity in the positions of the ionization zone within the acceleration channel.

### Hyperfine Spectral Structure

Of the 37 characterized isotopes of iodine, only 1 is naturally occurring, $^{127}$I.[2] As $^{127}$I contains an odd number of both neutrons and protons, each transition is further spin split due to nuclear magnetic dipole and electric quadrapole moments. Nuclei which have an odd number of protons and/or an odd number of neutrons possess an intrinsic nuclear spin $\mathbf{I}h/2\pi$, where $\mathbf{I}$ is integral or half-integral depending on if the atomic mass is even or odd, respectively[22] and boldface is used to denote vector quantities. For nuclei with non–zero nuclear spin (angular momentum, $\mathbf{J}$), the interaction of the nucleus with the bound electrons lead to the splitting of levels with $\mathbf{J}$ into a number of components, each corresponding to a specific value of the total angular momentum $\mathbf{F} = \mathbf{I} + \mathbf{J}$.[23] As a result of this interaction, $\mathbf{F}$ is a conserved quantity while $\mathbf{I}$ and $\mathbf{J}$ individually are not. The interaction is weak, al-



DISTRIBUTION A: Distribution Unlimited.

lowing the hyperfine splitting of each level to be taken independently of the other levels. The number of nuclear spin split hyperfine components is $2I+1$ if $J \geq 1$ and $2J+1$ if $J < 1$, with $F$ taking on the values $F = J+I, J+I-1, ..., |J-I|$ while satisfying the selection rules imposed on $F$, i.e. $\Delta F = 0, \pm 1$, unless $F = 0$, in which case $\Delta F \neq 0$.

With these selection rules on the quantum numbers for a particular electronic transition, and with knowledge of the hyperfine structure constants which characterize the magnetic dipole and electric quadrupole moments of the nucleus,[22] the hyperfine energy shifts from the position of the energy for the unshifted level with angular momentum $J$ can be easily calculated.[24,25] The relative intensities of transitions between these levels are derived assuming Russell–Saunders coupling,[24] allowing the complete construction of the fluorescence lineshape. Should there be more than on isotope, the intensities of the isotope shifted transitions are proportional to each isotopes relative abundance.

The relative intensities of the nuclear spin split hyperfine splitting are governed by two summation rules.[24] First, the sum of the intensities of all the lines of the hyperfine structure of a transition $J \rightarrow J'$ (the prime refers to the upper level involved in the transition) originating from a component $F$ of the level $J$ is proportional to the statistical weight of this component, $2F+1$. Second, the sum of the intensities of all the lines of the hyperfine structure, the transition $J \rightarrow J'$ ending on the component $F'$ of the level $J'$ is proportional to the statistical weight of this component, $(2F'+1)$. With these two sum rules, a system of linear equations is solved for the relative intensities of the nuclear spin split components of each isotope.

Two constants are associated with the magnitude of hyperfine nuclear spin splitting.[22] These are the $A$ hyperfine structure constant which represents the nuclear magnetic dipole effect on the atom, and the $B$ hyperfine structure constant which is associated with the nuclear electric quadrapole moment of the atom which will only be present if $I \geq 1$ . The relative energy of the spin split states depends on the sign of $A$ . In atoms with $A > 0$ , the state with the highest value of $F$ has the highest energy. While for atoms with $A < 0$, the state with the lowest value of $F$ has the highest energy.[24] The energy level shift $\Delta E_M$ associated with the magnetic dipole of the nucleus is given by Cowan.[22]

$$\Delta E_M(F) = \frac{1}{2}A[F(F+1)J(J+1)I(I+1)] = \frac{A}{2}C \quad (2)$$

Additionally, the energy spacing between successive levels $F-1$ and $F$ may be shown to be proportional to $F$.

$$\Delta E_M(F) - \Delta E_M(F-1) = AF \quad (3)$$

If $I \geq 1$, the nucleus will have an electric quadrapole moment and a related hyperfine splitting constant $B$ which produces an additional hyperfine splitting with energy linear in $C(C+1)$ where $C$ is previously defined in Eqn. 2.

$$\Delta E_F = \Delta E_M + \Delta E_Q \quad (4)$$

$$\Delta E_F = \frac{AC}{2} + \frac{B[\frac{3}{2}C(C+1)2I(I+1)J(J+1)]}{4I(2I-1)J(2J-1)} \quad (5)$$

Where $\Delta E_F$ is the combined nuclear spin split energy level shift combining the effect from the nuclear magnetic dipole moment $\Delta E_M$ and the effect of the electric quadrapole moment $\Delta E_Q$.[22] It should be noted that the center of gravity of the hyperfine levels lies at a position of the unsplit level $J$.[23]

$$\sum_F (2F+1)\Delta E_F \quad (6)$$

Due to close energy spacing of nuclear spin split levels, near ideal coupling between **I** and **J** occurs in most hyperfine structure. Therefore, the intensity $S$ rules derived by White for Russel–Saunders coupling are appropriate for hyperfine splitting.[24]

For $J-1 \rightarrow J$,

$F-1 \rightarrow F$:

$$S = \kappa \frac{(Q+I+1)(Q+I)(Q-I)(Q-I-1)}{F} \quad (7)$$

$F \rightarrow F$:

$$S = -\kappa \frac{(Q+I+1)(Q-I)(W+I)(W-I-1)(2F+1)}{F(F+1)} \quad (8)$$

$F+1 \rightarrow F$:

$$S = \kappa \frac{(W+I)(W+I-1)(W-I-1)(W-I-2)}{F+1} \quad (9)$$

For $J \rightarrow J$,

$F-1 \rightarrow F$:

$$S = -\kappa \frac{(Q+I+1)(Q-I)(W+I+1)(W-I)}{F} \quad (10)$$



DISTRIBUTION A: Distribution Unlimited.

$F \rightarrow F$:

$$S = \kappa \frac{[J(J+1) + F(F+1) + I(I+1)]^2 (2F+1)}{F(F+1)} \tag{11}$$

$F + 1 \rightarrow F$:

$$S = -\kappa \frac{(Q+I+2)(Q-I+1)(W+I)(W-I-1)}{(F+1)} \tag{12}$$

Where $S$ is the transition strength and $\kappa$ is an arbitrary constant. The variables $Q = J + F$ and $W = J - F$ are only introduced to compress the notation.

The relative intensities of the isotope shifted transitions are proportional to each isotope's relative abundance. However, the relative intensities of the nuclear spin split hyperfine splitting are governed by two summation rules.[23] First, the sum of the intensities of all the lines of the hyperfine structure of a transition $J \rightarrow J'$ originating from a component $F$ of the level $J$ is proportional to the statistical weight of this component, $(2F + 1)$. Second, the sum of the intensities of all the lines of the hyperfine structure the transition $J \rightarrow J'$ ending on the component $F'$ of the level $J'$ is proportional to the statistical weight of this component, $(2F' + 1)$. With these two sum rules, a system of linear equations are solved for the relative intensities of the nuclear spin split components of each isotope.

The practical issues associated with hyperfine isotopic spin splitting in the measurements of plasma acceleration in the plume and within Hall effect thrusters are that it may create much more complex transition structure in high resolution. To some extent, hyperfine spin splitting can be neglected for some transitions, especially when the spacing between the spin split components is small. From previous studies when LIF was used in the plumes of Hall effect thrusters, the $5d[4]_{7/2} - 6p[3]_{5/2}$ spin split electronic transition of Xe II at 834.72 nm is relatively narrow at approximately 500 MHz and the hyperfine structure can be neglected to a large degree in analysis of Hall effect thruster plasma dynamics.[26,27] In contrast, the Xe I $6s[3/2]^0_2 - 6p[3/2]_2$ transition at 823.18 nm is dramatically broader and visually more complex due to the spin split odd isotopes.[25]

Iodine, with its single naturally occurring isotope, requires us to only examine a single isotope, albeit with the added complexity of the hyperfine spectra. With the nuclear spin of $^{127}$I at $\frac{5}{2}$,[2] $5d^5D^o_4$–$6p^5P_3$ transition is spin split into 15 components as shown in Fig. 3. Knowledge of **I** and **J** for each state allow us to calculate **F**. From Russell-Saunders (L–S) coupling we are able to estimate the relative intensity of the hyperfine spin–split components as shown in Fig. 3.

We have not been able to find values for $A$ and $B$ for the $5d^5D^o_4$–$6p^5P_3$ transition in the limited literature for the second spectrum of iodine. As such, the spacing of the hyperfine spectral components is unknown. Since the transition does not involve an $s$ orbital, it is less likely that the hyperfine spectral will be particularly broad.[24] The theoretical wider breadth of $s$–orbital transitions is consistent with observations of neutral xenon by Cedolin[25] and of singly ionized bismuth by Scharfe.[28] It should be noted that in Fig. 3 the value of $A$ for each state is assumed positive. Negative values of $A$ would invert the energies of the spin–split states $(F)$ shown in Fig. 3.

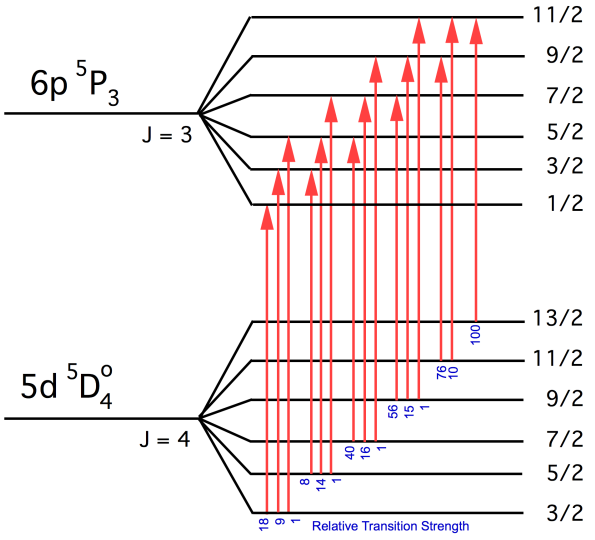


**Fig. 3 Hyperfine spin splitting of the $5d^5D^o_4$–$6p^5P_3$ at 695.878 nm. Note estimated relative line strengths shown in blue for each hyperfine transition.**

## Experimental Efforts

With an identified, and to the best extent possible, characterized ionic iodine transition, we have begun the process of developing a table–top apparatus to experimentally characterize our analysis of the relevant iodine transition. This effort seeks to verify the spectroscopy presented and determine how it can be best applied to an accelerated iodine ion beam. This section presents the results in our development of a table top microwave iodine plasma discharge. It also references related work occurring at the Busek Company where the visible and NIR spectrum of a low power iodine Hall effect thruster was measured. Finally, initial laser source selection is discussed including the possible need for increased sensitivity in the detection apparatus.

### Iodine Microwave Plasma Discharge

As most glow discharge lamps are only weakly ionized, we chose to use a 2.45 GHz microwave with



DISTRIBUTION A: Distribution Unlimited.

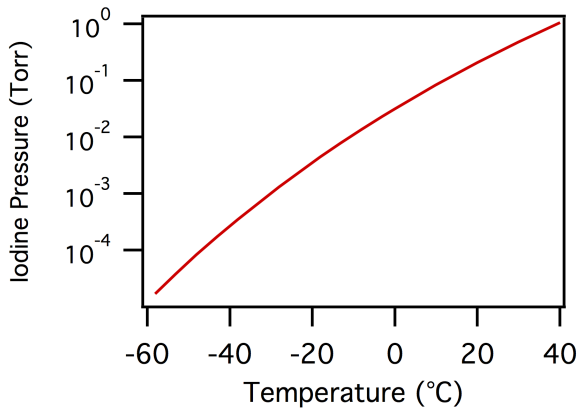


**Fig. 4 Partial pressure of iodine gas as a function of pressure.**

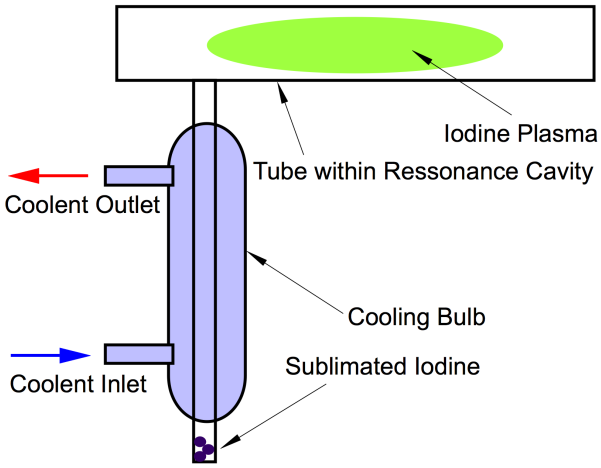


**Fig. 5 Variable pressure, closed cell iodine microwave discharge lamp diagram.**

an Evanson microwave resonant cavity supplied by Opthos Instruments, Inc.[29] The tuned cavity allows for the efficient coupling of 2.45 GHz radiation to either stationary or flowing gas at pressures ranging from a few milli-Torr to several hundred Torr. Lamp geometries are typically a sealed glass, or quartz, cylinder 25 mm in diameter, and 100 mm long.

Our first iodine discharge lamp consisted of several mg of iodine and 3 mTorr neon fill in enhance lamp stability. The partial pressure of the iodine was varied using a 50 mm long, 6 mm diameter cold finger, immersed in a ice bath. By varying the temperature it is possible to precisely vary the iodine partial pressure. The iodine pressure as a function of temperature is given in Eqn. 13 and graphically shown in Fig. 4.

$$\log_{10} P = 18.8 - \frac{3594}{T} + 0.00044T - 2.98 \log_{10} T \quad (13)$$

Where $T$ is temperature in Kelvin and the $P$ is the iodine partial pressure in Torr.[30] There were several issues with this first spectral source. First, the lamp produced strong neon neutral emission at 692.9, 702.4, and 703.2 nm. Although the neon emission features required caution at high detector gain, they are sufficiently distant from the $5d^5D_4^o$–$6p^5P_3$ transition at 695.878 nm as to not blend. However, the short iodine cold finger required immersion in an ice bath and it was difficult to adequately control temperature, and we were unable to maintain temperatures below approximately 5 °C.

As a result of the inability to reach temperatures less than 5 °C, the iodine pressure within the lamp envelope remained above 50 milli-Torr. From the studies of the second spectrum of iodine by Martin and Corliss,[13] iodine pressures of less than 10 mTorr were required to produce substantial iodine ion emission. The 300 mTorr argon fill likely does not enhance iodine ionization via the Penning effect since argon's first excited state is only 10.5 eV, and it may alternatively quench iodine ions if the total pressure is too high. It is useful to note that Martin and Corliss used a water jacketed lamp without any fill gases; however, their lamps were prone to poisoning due to intrusion of atmospheric gases.

As a result of our experiences with the first lamp, we designed a second custom lamp from Opthos Instruments, Inc. A schematic of this lamp is shown in Fig. 5. This lamp contained a vacuum ($< 10^{-4}$ Torr) with several mg of iodine. The most important change was the addition of an integral glass cooling bulb on the cold finger. This allows precise cooling of the discharge cold finger using a 50:50 water-glycol laboratory chiller. We have achieved steady temperatures of -12 °C with a 25 W plasma discharge. This corresponds to an iodine pressure of approximately 8 mTorr.

A photograph of the redesigned discharge lamp operating at 30 °C is shown in Fig. 6. Note the blue discharge. As the temperature is lowered and the pressure of iodine is lowered as per Eqn. 13, the discharge becomes more diffuse, but also exhibits a green hue.

Figure 7 shows the temperature dependency of the intensity of the iodine ion $5d^5D_4^o$–$6p^5P_3$ transition at 695.878 nm as a function of side arm temperature. There is virtually no signal above 15 °C; however below this temperature, the signal grows monotonically. The signal rises linearly to the minimum temperature achievable with our apparatus of -12.5 °C. With decreased temperatures, we believe that we may further increase the signal strength by an additional 50%. It should be noted that Martin and Corliss were not able to ignite their lamp at temperatures less that −25 °C which corresponds to a iodine partial pressure of approximately 350 mTorr.[13] Others have reported significantly iodine ion populations at −25 °C using a helium–iodine Penning mixture.[30] We plan to continue our investigations of temperature dependance to maximize the metastable $5d^5D_4^o$ state population for



DISTRIBUTION A: Distribution Unlimited.

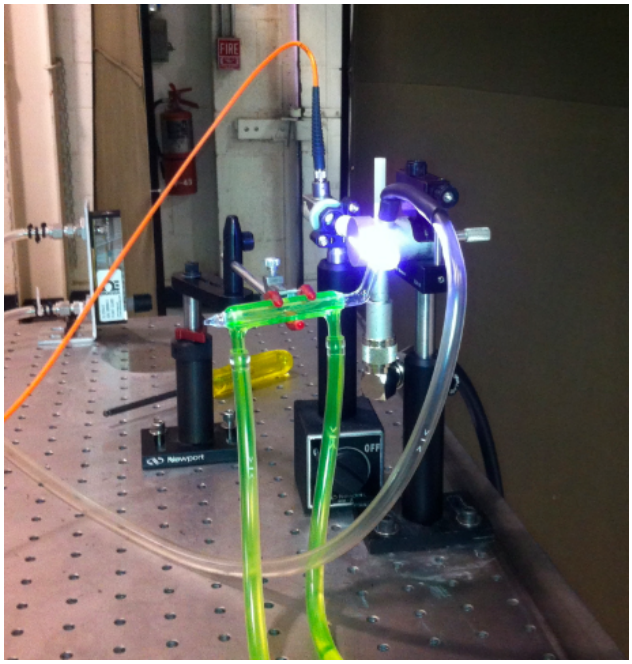

**Fig. 6 Variable pressure, closed cell iodine microwave discharge lamp with 25 W plasma discharge. Note Glycol cooling lines (green) maintaining temperature of iodine cold finger, clear plastic tubing for dry air purge, and orange clad fiber optic cable.**

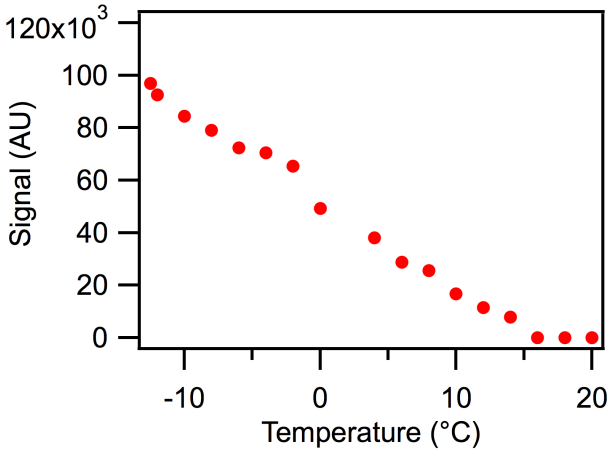


**Fig. 7 Intensity of the iodine ion $5d^5D_4^o$–$6p^5P_3$ transition at 695.878 nm as a function of side arm temperature.**

active probing. It may also be in our interest to investigate whether a helium Penning mixture (helium's first excited state is 19.8 eV) will increase the population of our metastable iodine ion.

Future efforts with the discharge lamp may include possible introduction of helium, or neon (neon's first excited state is 16.6 eV), to enhance ionization of iodine via the Penning effect. Helium rather than neon may be more effective due its the first excited state being greater than 20 eV above the ground state and the

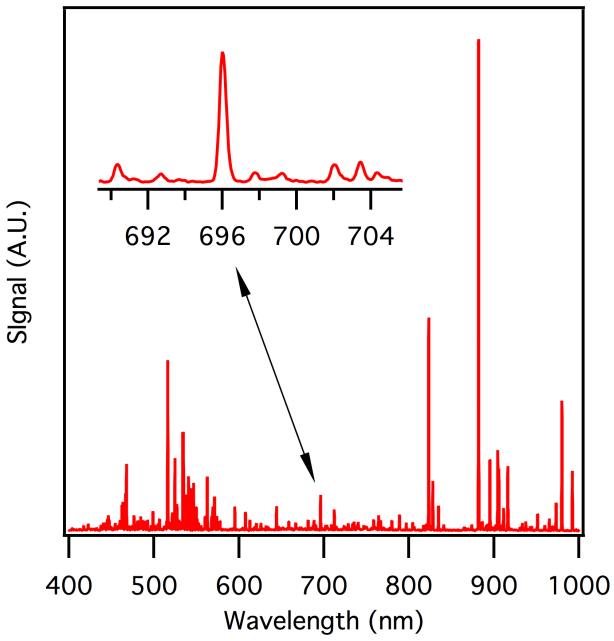


**Fig. 8 Emission from a 200 W Hall effect thruster plume centerline taken approximately 1 thruster diameter downstream of exit plane. Data provided by Prince and Chiu.[31]**

lack of any transitions near those of iodine near 696 and 516 nm which appear to be most of interest. One reference indicates that partial pressures of helium as high as 300 mTorr with iodine partial pressure of a few mTorr would be advantageous.[30] This is an active avenue for future investigation.

### Hall Thruster Plume Emission: Related Research

While investigations of iodine propellant for electrostatic plasma thrusters has been extremely limited, recent exploratory work at the Busek Co in Natick, MA has performed a number of measurements of an iodine Hall effect thruster.[9,10,31] These measurements have focused primarily on performance verification and identification of species produced by the thruster. As a result, applied diagnostics have been focused on measuring performance and determining spacecraft integration issues such as plume divergence.[9,10] However, more recent measurements of optical emission performed by Prince and Chiu have captured the optical emission in the visible and NIR for a low power Hall effect thruster as shown in Fig. 8.

The Hall effect thruster emission in Fig. 8 also contains substantial xenon emission, particularly evident in the NIR (e.g. 823 nm and 890 nm). For example the lines at 823 and 828 nm are xenon neutral lines. This xenon spectrum is due to hollow cathode operation on xenon during these preliminary tests where iodine was only run through the anode discharge.

As stated previously, the $5d^5D_4^o$–$6p^5P_3$ transition at 695.878 nm, the upper $5p^5P_3$ state has three strong



DISTRIBUTION A: Distribution Unlimited.

radiative decay paths previously identified. These are at 540.542 nm to $5p^5\ {}^3P_2^o$ state, 681.257 nm to $5d^5D_3^o$ state, and 516.12 nm to $6s^5S_2^o$ state. From Prince and Chiu's data the relative ratios of emission (relative to the 695.878 nm line are 1.5, 0.3, and 4.8, respectively. These values are similar to ratios of measured by Martin and Corliss of 0.8, 4, and 3, respectively, with the notable exception of the 681.257 nm line to the $5d^5D_3^o$ state. This substantial difference may be due to the very high ionization fraction (90% by flux, and 50% by density) that characterizes a Hall effect thruster discharge. It is interesting to note that for the purpose of survey spectroscopy of the second spectra of gaseous plasma species; a Hall effect thruster is likely much superior over the Geissler tubes of yore.

**Laser Spectroscopy: Future Work**

We are presently evaluating various lasers for interrogating the $5d^5D_4^o$–$6p^5P_3$ transition at 695.878 nm. Ultimately, our preferred laser platform would be based on an external cavity diode laser, such as those that have been used in previous studies in our lab.[32,16] However, commercially available single mode diode lasers have also been successfully used in the past.[33,25] Such lasers provide a significantly less expensive laser source capable of scanning across 20 GHz, or more. It should be noted that the line widths of commercial laser diodes are 15–30× broader than external cavity systems. However, the lower cost and ease of working with commercial laser diodes makes these systems preferred for exploratory measurements such as these.

At present, we are evaluating the commercially available diode laser inventory for tunability about 695.878 nm (air) wavelength. As there is considerable batch to batch variability in diode laser production, finding commercial diodes that lase at the appropriate wavelength requires testing until a suitable batch is identified.

The 2.45 GHz microwave resonance lamp previously described will be our source of choice. However, we are also investigating construction of a opto-galvanic cell based on a commercial atomic emission hollow cathode lamp. Use of a opto-galvanic cell would increase measurement sensitivity significantly, but at the likely expense of decreased number density of the $5d^5D_4^o$ $I^+$ state. Present studies are examining the compatibility of iodine (most likely in a helium Penning mixture) on the components of a commercial hollow cathode lamp.

## Conclusions and Future Efforts

We have presented background research to identify a metastable transition of $I^+$ suitable for LIF interrogation for measurement of iodine plasma acceleration, specifically for characterizing electrostatic plasma propulsion thrusters. We have identified the $I^+$ $5d^5D_4^o$ state as metastable and therefore likely to have a large population. We have also identified the $5d^5D_4^o$–$6p^5P_3$ transition at 695.878 nm as the best candidate transition based on the limited available spectral data. From the $6p^5P_3$ upper state of this transition, the $6s^5S_2^o$–$6p^5P_3$ transition at 516.12 nm appears to be the best candidate for non-resonant fluorescence collection with a branching ratio of between 30 to 70%. Data, provided courtesy of the Busek Company, clearly shows that the transitions are interest are evident in plume emission in the plume of a low power Hall effect thruster.

We have constructed a new discharge lamp that allows for the variation of the iodine pressure via active temperature control. The transitions of interest have been identified in our microwave table top discharge and we feel that a substantial population of the $I^+$ $5d^5D_4^o$ metastable state is present. We are also presently working on identifying suitable laser sources to continue our tabletop experimental effort in order to confirm our spectroscopic model. We have excellent reasons to believe that the hyperfine spectra will be complex, but will not be exceptionally broad. It is therefore imperative that we confirm our calculations via tabletop experimentation prior assembling a full scale LIF velocity measurement apparatus.

Signal strength of absorption and LIF in the lamp may require further modification of our microwave discharge lamp. A Penning mixture of either neon or helium may significantly enhance our iodine ionization fraction. We are also contemplating more sensitive laser measurement techniques, specifically opto-galvanic spectroscopy. One significant benefit of an opto-galvanic cell is that it may also be used as an easily implemented stationary reference for LIF velocimetry of an accelerated plasma plume should we implement our LIF velocimetry system as envisioned.

The development of iodine specific laser diagnostics to iodine plasma acceleration in electro-static plasma thrusters, especially Hall effect thrusters, appears to have justification due to large price fluctuations for xenon as well as limited production. In some cases, especially orbit maintenance, the use of iodine fuels may offer distinct advantages of low pressure, high storage density. Ultimately iodine will essentially provide the benefits of cryogenic storage of xenon and krypton propellants without the need for expensive and complex cryogenic systems.

## Acknowledgments

The authors would like to thank the staff of Opthos Instruments for their patience and many fruitful discussions in the development of the iodine microwave discharge lamp. Also, thanks are due to Drs. Chiu and Szabo of the Busek Company, and Dr. Prince of AFRL/RVBXT, for their assistance in providing the iodine spectra and performance data from a low power Hall effect thruster. The authors are also very much indebted to several *classically OCD* AFRL colleges.



DISTRIBUTION A: Distribution Unlimited.

# References


[1]R. Jahn, *Physics of Electric Propulsion.* McGraw-Hill, 1968.

[2]D. R. Lide, *Handbook of Chemistry and Physics*, 79th ed. CRC Press, 1998.

[3]O. Duchemin, D. Valentian, and N. Cornu, "Cryostorage of propellants for electric propulsion," in *Proceedings of the 45th Joint Propulsion Conference and Exhibit*, no. AIAA-2009-4912. American Institute of Aeronautics and Astronautics, August 2009.

[4]D. Jacobson and D. Manzella, "50 kw class krypton hall thruster performance," in *Proceedings of the 39th Joint Propulsion Conference and Exhibit*, no. AIAA-2003-4550. Huntsville, AL: American Institute of Aeronautics and Astronautics, July 2003.

[5]J. A. Linnell and A. D. Gallimore, "Efficiency analysis of a hall thruster operating with krypton and xenon," *Jounrnal of Propulsion and Power*, vol. 22, no. 6, pp. 1402–1418, November-December 2006.

[6]M. R. Nakles, W. A. Hargus, J. J. Delgado, and R. L. Corey, "A performance comparison of xenon and krypton propellant on an spt-100 hall thruster," in *Proceedings of the 32nd International Electric Propulsion Conference*, no. 003. Weisbaden, Germany: Electric Rocket Society, September 2011.

[7]R. Dressler, Y. Chiu, and D. J. Levandier, "Propellant alternatives for ion and hall effect thrusters," in *Proceedings of the 38th Aerospace Sciences Meeting and Exhibit*, no. AIAA-2000-0602. Reno, NV: American Institute of Aeronautics and Astronautics, January 2000.

[8]O. Tverdokhlebov and A. V.Semenkin, "Iodine propellant for electric propulsion: To be or not to be," in *Proceedings of the 37th Joint Propulsion Conference and Exhibit*, no. AIAA-2001-3350. Salt Lake City, UT: American Institute of Aeronautics and Astronautics, July 2001.

[9]J. Szabo, B. Pote, S. Paintal, M. Robin, G. Kolencik, A. Hillier, R. Branam, and R. Huffman, "Performance evaluation of an iodine vapor hall thruster," in *Proceedings of the 47th Joint Propulsion Conference and Exhibit*, no. AIAA-2011-5891. San Diego, CA: American Institute of Aeronautics and Astronautics, Auguste 2011.

[10]A. C. Hillier, "Revolutionizing space propulsion through the characterization of iodine as fuel for hall-effect thrusters," Master's thesis, Air Force Insistute of Technology, Wrght-Patterson AFB, March 2011.

[11]L. Dorf, Y. Raistes, and N. J. Fisch, "Electrostatic probe apparatus for measurements in the near-anode region," *Review of Scientific Instruments*, vol. 75, no. 5, pp. 1255–1260, May 2004.

[12]W. A. Hargus Jr., "Laser-induced fluorescence measurements of neutral xenonin the near field of a 200 w hall thruster," in *Proceedings of the 41st Joint Propulsion Conference and Exhibit*, no. AIAA-2005-4400. Tucson, AZ: American Institute of Aeronautics and Astronautics, July 2005.

[13]W. Martin and C. H. Corliss, "The spectrum of single ionized atomic iodine ( i ii)," *Journal of Research of the National Bureau of Standards A*, vol. 64A, no. 6, pp. 443–479, November-December 1960.

[14]Y. Ralachenko, A. E. Kramida, J. Reader, and N. A. Team. Nist atomic spectra data base version 4.1.0.

[15]W. A. Hargus Jr. and M. A. Cappelli, "Laser-induced fluorescence measurements of velocity within a hall discharge," *Applied Physics B*, vol. 72, no. 8, pp. 961–969, June 2001.

[16]W. A. Hargus and C. S. Charles, "Near exit plane velocity field of a 200 w hall thruster," *Journal of Propulsion and Power*, vol. 24, no. 1, pp. 127–133, January-February 2008.

[17]S. Mazouffre, D. Gawron, V. Kulaev, and N. Sadeghi, "A laser spectroscopic study on xe+ ion transport phenomena in a 5 kw-class hall effect thruster," in *Proceedings of the 30th International Electric Propulsion Conference*, no. IEPC-2007-160. Florence, Italy: Electric Rocket Society, September 2007.

[18]W. Demtroder, *Laser Spectroscopy: Basic Concepts and Instrumentation.* Springer-Verlag, 1996.

[19]M. R. Nakles and W. A. Hargus Jr., "Background pressure effects on internal and near-field ion velocity distribution of the bht-600 hall thruster," in *Proceedings of the 44th Joint Propulsion Conference and Exhibit*, no. AIAA-2008-5101. Hartford, CT: American Institute of Aeronautics and Astronautics, July 2008.

[20]W. A. Hargus Jr., M. R. Nakles, B. Pote, and R. Tedrake, "The effect of thruster oscillations on axial velocity distributions," in *Proceedings of the 44th Joint Propulsion Conference and Exhibit*, no. AIAA-2008-4724. Hartford, CT: American Institute of Aeronautics and Astronautics, July 2008.

[21]T. Fujimoto and A. Iwamae, Eds., *Plasma Polarization Spectroscopy*, ser. Series on Atomic, Optical and Plasma Physics. Springer-Verlag, 2008, vol. 44.

[22]R. D. Cowan, *The Theory of Atomic Structure and Spectra.* Berkeley, CA: University of California Press, 1981.

[23]I. I. Sobelman, *Atomic Spectra and Radiative Transitions.* Berlin: Springer-Verlag, 1992.

[24]H. E. White, *Introduction to Atomic Spectra.* New York: McGraw-Hill, 1934.

[25]R. Cedolin, "Laser-induced fluorescence diagnostics of xenon plasmas," Ph.D. dissertation, Stanford University, June 1997.

[26]W. A. Hargus and C. S. Charles, "Near-plume laser-induced fluorescence velocity measurements of a medium power hall thruster," *Journal of Propulsion and Power*, vol. 26, no. 1, pp. 135–141, January-February 2010.

[27]W. A. Hargus Jr. and M. R. Nakles, "Evolution of the ion velocity distribution in the near field of the bht-200-x3 hall thruster," in *Proceedings of the 42nd Joint Propulsion Conference and Exhibit*, no. AIAA-2006-4991. Sacramento, CA: American Institute of Aeronautics and Astronautics, July 2006.

[28]D. B. Scharfe, "Alternative hall thruster propellants krypton and bismuth: Simulated performance and characterization," Ph.D. dissertation, Stanford University, Palo Alto, CA, August 2009.

[29]F. C. Fehsenfeld, K. M. Evanson, and H. P. Broida, "Microwave discharge cavities operating at 2450 mhx," *Review of Scientific Instruments*, vol. 36, no. 3, p. 294, March 1965.

[30]A. Kono and S. Hattori, "Radiative-lifetime measurements for i i and i ii," *Journal of the Optical Socienty of America*, vol. 69, no. 2, pp. 253–255, February 1979.

[31]B. Prince and Y. Chiu, "Optical emission spectra of the iodine hall thruster," in *Proceedings of the 48th Joint Propulsion Conference and Exhibit*, no. AIAA-2010-xxxx. Atlanta, GA: American Institute of Aeronautics and Astronautics, August 2012.

[32]W. A. Hargus, G. M. Azarnia, and M. R. Nakles, "Demonstration of laser-induced fluorescence on a krypton hall effect thruster," in *Proceedings of the 32nd International Electric Propulsion Conference*, no. IEPC-2011-018. Electric Rocket Society, September 2011.

[33]D. H. Manzella, "Stationary plasma thruster ion velocity distribution," in *Proceedings of the 30th Joint Propulsion Conference and Exhibit*, no. AIAA-1994-3141. American Institute of Aeronautics and Astronautics, June 1994.




DISTRIBUTION A: Distribution Unlimited.